

Heat flux and shear rate in turbulent convection

Emily S. C. Ching

Department of Physics, The Chinese University of Hong Kong, Shatin, New Territories, Hong Kong

(Received 8 August 1995; revised manuscript received 14 May 1996)

One interesting feature of hard turbulence, a scaling regime in turbulent convection, is the presence of a large-scale mean circulating flow. Its effect on heat flux was studied by Shraiman and Siggia [Phys. Rev. A **42**, 3650 (1990)], who approximated it as a shear flow near the boundaries. A constant shear rate was considered, which, in effect, assumes that heat is carried mainly by the mean flow. Experiments indicate, however, that a significant portion of heat is carried by the thermal plumes. In this paper, an analysis for a position-dependent shear rate is presented. The relation between the heat flux and the shear rate is found to depend crucially on the shape of the temperature profile. For the general profile that remains the same throughout a range of Rayleigh numbers, the relation is different from the previous result and agrees better with some recent experimental observations. [S1063-651X(97)05201-X]

PACS number(s): 47.27.Te, 47.27.Nz

Experimental studies of Rayleigh-Bénard convection have revealed a scaling state, known as hard turbulence, which covers a wide range of Rayleigh number Ra , from 10^8 to 10^{15} [1]. In this turbulent regime, the measured quantities, e.g., heat flux and the size of local temperature fluctuations, all exhibit a power-law dependence on Ra . Particularly interesting is the observed scaling exponent of the heat flux being different from the “classical” value that one would obtain from marginal stability arguments [2]. Another unexpected feature is the presence of a large-scale circulating flow that spans the whole experimental cell [3]. The mean velocity also scales with Ra .

Hard turbulence is believed to be described by the following equations [4] of an incompressible fluid:

$$\frac{\partial \vec{u}}{\partial t} + \vec{u} \cdot \vec{\nabla} \vec{u} = -\vec{\nabla} p + \nu \nabla^2 \vec{u} + g \alpha T \hat{z}, \quad (1a)$$

$$\frac{\partial T}{\partial t} + \vec{u} \cdot \vec{\nabla} T = \kappa \nabla^2 T, \quad (1b)$$

$$\vec{\nabla} \cdot \vec{u} = 0, \quad (1c)$$

where \vec{u} is the velocity field, p the pressure divided by density, T the temperature field, and \hat{z} the unit vector in the vertical direction. In Eq. (1), g is the acceleration due to gravity; α , ν , and κ are, respectively, the volume expansion coefficient, kinematic viscosity, and thermal diffusivity of the fluid. There are two dimensionless parameters: $Ra = \alpha g \Delta L^3 / \nu \kappa$, where Δ is the applied temperature difference and L is the height of the cell, and the Prandtl number Pr , which is the ratio ν / κ .

When convective turbulence occurs, the center is statistically isothermal as the fluctuating velocity field smooths out any temperature gradient. However, the velocity field vanishes at the top and bottom plates because of the no-slip boundary condition, so heat can be transported only by conduction there. As a result, the temperature difference concentrates in two regions, i.e., two thin thermal boundary layers are developed, across which heat is transported mainly by

conduction. Using the vertical temperature gradient, one can define a thermal boundary layer thickness λ ,

$$\lambda(x) \equiv \frac{\Delta/2}{\left| \frac{\partial T}{\partial z} \right|_{z=0}}, \quad (2)$$

across which half the temperature difference drops. The coordinates are defined with $z=0$ at the bottom plate.

Heat flux transferred across the cell is given by the Nusselt number Nu , which is the actual heat flux normalized by that transported if there were only conduction. We can also define a pointwise Nusselt number Nu_{pt} as

$$Nu_{pt}(x) \equiv \frac{k \sigma \left| \frac{\partial T}{\partial z} \right|_{z=0}}{k \sigma \frac{\Delta}{L}} = \frac{L}{2\lambda(x)}, \quad (3)$$

where k is the thermal conductivity of the fluid and σ is the cross-sectional area of the cell. It has been found experimentally [5] that $Nu_{pt}(x)$ has the same scaling as Nu when x is at the middle of the cell. Since we are interested only in scaling properties in this paper, we shall estimate Nu by Nu_{pt} at $x=L/2$, which is in the middle of an aspect-ratio-one cell. The problem of understanding the scaling of Nu thus becomes a question of how thick the thermal boundary layer should be.

A classical model [2] argues that the boundary layer maintains its thickness such that it is marginally stable against convection. This idea implies that the Rayleigh number of the boundary layer $Ra_\lambda = \alpha g \Delta \lambda^3 / 2 \nu \kappa$ would be at the fixed critical value for the onset of convection. This leads to $\lambda/L \sim Ra^{-1/3}$, which translates to $Nu \sim Ra^{1/3}$. As pointed out by others [6], this result does not, however, agree with the experimental observation $Nu \sim Ra^{0.285 \pm 0.004}$ [1]. Several models have been proposed to explain this nonclassical scaling in Nu [6–8].

In Ref. [6], it was assumed that there are essentially three different regions inside the cell: (i) a well-mixed central re-

gion, (ii) the top and bottom boundary layers, and (iii) an in-between plumes-dominated mixing layer. Different terms in Eq. (1a) were then balanced in an order-of-magnitude fashion in the various regions. This analysis yielded a scaling in Nu, $Nu \sim Ra^{2/7} Pr^{-1/7}$, which agrees well with the experimental result. However, the model implicitly assumed that heat flux is mainly transferred convectively through the central region, which is not what has been observed experimentally [5] and numerically [9].

The existence of a large-scale mean circulating flow was found in further experimental measurements. Such a large-scale flow generates velocity boundary layers at the walls. Its effect on the heat flux was studied by Shraiman and Siggia, who analyzed the interaction between the thermal and velocity boundary layers [8]. They approximated the large-scale flow by a shear near the boundaries and considered the shear rate γ to be constant. They found

$$Nu \sim \left(\frac{\gamma L^2}{\kappa} \right)^{1/3}. \quad (4)$$

Using empirically verified results for the shear rate of a turbulent velocity boundary layer and the kinetic-energy dissipation in turbulent shear flows in pipes or channels, they again reproduced the observed scaling in Nu.

Several experimental studies of the thermal and velocity boundary layers [5,10–12] have been performed and, as a result, new questions are raised. Firstly, experiments indicate that the observed $2/7$ scaling in Nu starts already at some Ra when the velocity boundary layer is not yet turbulent [12]. This is puzzling as the shear rate and the kinetic-energy dissipation should be quite different for a laminar velocity boundary layer. Second, considering a constant shear rate implicitly assumes that the heat flux is mainly carried by the large-scale mean flow, but experimental observation showed that a significant portion of heat is carried by the thermal plumes [5]. Finally, and more importantly, Eq. (4) cannot be verified by some recent direct velocity measurements [13], which found instead

$$\frac{\gamma_0 L^2}{\kappa} \sim Ra^{0.66 \pm 0.01}, \quad (5)$$

$$Nu \sim \left(\frac{\gamma_0 L^2}{\kappa} \right)^{0.44}, \quad (6)$$

where γ_0 is the shear rate measured near the bottom plate in the middle of the cell. Chilla *et al.* [14] reported experimental evidence that Eq. (4) is correct, but no direct shear rate measurements were made in their work. Werne [15] reported that Eq. (4) is consistent with the data obtained in two-dimensional numerical simulations.

In this paper, an analysis for nonuniform shear rate is presented. The shear rate $\gamma(x)$ is now a function of position. The relation between the shear rate and the heat flux is found to depend crucially on the shape of the temperature profile. For the general temperature profile that remains the same throughout a range of Ra, the relation is different from Eq. (4) and agrees better with Eq. (6).

The horizontal velocity is taken to be $u_x = \gamma(x)z$. Then $u_z = -\gamma'(x)z^2/2$, where the prime indicates a derivative

with respect to x . Since the vertical velocity u_z is not neglected, heat carried by the thermal plumes [16] is effectively taken into account. The time-independent heat equation

$$\gamma(x)z \frac{\partial T}{\partial x} - \frac{\gamma'(x)z^2}{2} \frac{\partial T}{\partial z} = \kappa \frac{\partial^2 T}{\partial x^2} + \kappa \frac{\partial^2 T}{\partial z^2} \quad (7)$$

is then solved for a class of $T(x, z)$, which has a self-similar form

$$\frac{T(x, z) - T_{\text{bot}}}{\Delta} = -\zeta \left(\frac{z}{\lambda(x)} \right) \quad (8)$$

and satisfies

$$\zeta(0) = 0, \quad \zeta(\infty) = \frac{1}{2}, \quad \zeta^{(1)}(0) = \frac{1}{2}. \quad (9)$$

The notation $\zeta^{(n)}$ denotes the n th derivative of ζ with respect to its argument. Conditions in Eq. (9) ensure, respectively, $T(x, z) = T_{\text{bot}}$ at $z = 0$, where T_{bot} is the temperature of the lower plate, half of the temperature difference drops across the bottom boundary layer, and consistency with Eq. (2). The function ζ is the normalized temperature profile whose vertical distance is measured in units of the thermal boundary layer thickness $\lambda(x)$. This class of solutions is considered because numerical simulations have found that the average temperature profile is well approximated by such a form [15]. The temperature profile obtained in Ref. [8] also belongs to such class.

Substituting Eq. (8) into Eq. (7) results in an ordinary differential equation for $\zeta(p)$:

$$\begin{aligned} & -p^2 \zeta^{(1)}(p) \frac{[\gamma(x)\lambda^2(x)]'}{2\kappa\lambda(x)} \\ & = p \zeta^{(1)}(p) \left\{ \frac{2[\lambda'(x)]^2 - \lambda''(x)\lambda(x)}{\lambda^2(x)} \right\} \\ & \quad + p^2 \zeta^{(2)}(p) \left[\frac{\lambda'(x)}{\lambda(x)} \right]^2 + \zeta^{(2)}(p) \frac{1}{\lambda^2(x)}, \end{aligned} \quad (10)$$

where $p = z/\lambda(x)$. A solution for Eq. (10) exists if and only if the functions of x in all the terms are proportional to each other [17]. This implies

$$\lambda'(x) = K, \quad \frac{\lambda(x)[\gamma(x)\lambda^2(x)]'}{2\kappa} = A, \quad (11)$$

where K and A are constants independent of x , but may depend on Ra. A constant γ would lead to the conclusion that $\zeta^{(2)}(p) = 0$, which is not allowed. With Eq. (11), Eq. (10) becomes

$$-(2K^2p + Ap^2)\zeta^{(1)}(p) = (1 + K^2p^2)\zeta^{(2)}(p),$$

whose solution depends on whether or not K and A vanish.

We first consider the case when both K and A are nonzero and find

$$\zeta(p) = \frac{1}{2} \int_0^p \frac{\exp\left\{-\frac{A}{K^3}[Kq - \arctan(Kq)]\right\}}{1 + K^2 q^2} dq, \quad (12)$$

where A and K are related by $\zeta(\infty) = 1/2$. Thus the normalized temperature profile is determined up to one constant, which we take to be K for definiteness. Moreover, $K^2 = -\zeta^{(3)}(0)$ and $A = -\zeta^{(4)}(0)$. Equation (11) leads to $\lambda(x) = Kx + c$, where c is a constant, and

$$\frac{\gamma_0 L^2}{\kappa} \sim \frac{8A(K)}{K} \text{Nu}^2 (\ln \text{Nu}). \quad (13)$$

The constant K might be a function of Ra . However, if the shape of the normalized temperature profile near the middle of the cell remains the same over a certain range of Ra , then K is a constant independent of Ra in this range. Equation (13) then implies that $\gamma_0 L^2/\kappa$ scales like $\text{Nu}^2 (\ln \text{Nu})$ in this range of Ra . There is numerical evidence [15] that the normalized temperature profile near the middle region of the cell has the same shape for the range of Ra studied.

Next, consider the case $K=0$ but $A \neq 0$. We have

$$\zeta(p) = \frac{1}{2A^{1/3}} \int_0^{A^{1/3}p} e^{-q^{3/3}} dq, \quad A = 2.13622. \quad (14)$$

Note that Eq. (14) is the $K \rightarrow 0$ limit of Eq. (12) and resembles the temperature profile obtained by Shraiman and Siggia [8]. Moreover,

$$\frac{\gamma_0 L^2}{\kappa} \sim 16A \text{Nu}^3, \quad (15)$$

which agrees with the prediction [Eq. (4)] of Ref. [8].

Finally, for $A=0$ but $K \neq 0$,

$$\zeta(p) = \frac{1}{2K} \arctan(Kp), \quad (16)$$

with $K = \pi/2$ and

$$\frac{\gamma_0 L^2}{\kappa} \sim 8B \text{Nu}^2, \quad (17)$$

which implies that the shear rate scales like Nu^2 if the constant B does not depend on Ra .

Hence the relation between the shear rate and the heat flux depends crucially on the normalized temperature profile $\zeta(p)$. In Fig. 1 we plot $\zeta(p)$ for the three cases: (i) $K \approx A \approx 1$, (ii) $K=0$ and $A=2.13622$, and (iii) $A=0$ and $K = \pi/2$. The profile for $A=0$ is much broader than the profiles reported in the literature [12,15], implying that the relation between the shear rate and the heat flux would not be given by Eq. (17).

The observation of $\gamma_0 L^2/\kappa \sim \text{Nu}^3$ in two-dimensional numerical simulations [15] suggests that the normalized temperature profiles correspond to $K \approx 0$. This is supported by a good resemblance of Fig. 1 and Fig. 15(d) in Ref. [15] and by a direct estimate of the slope of $\lambda(x)$ for $0 < x < L/2$ from Fig. 16(d) in [15]. On the other hand, Fig. 3 in Ref. [12] shows two experimental normalized temperature profiles for

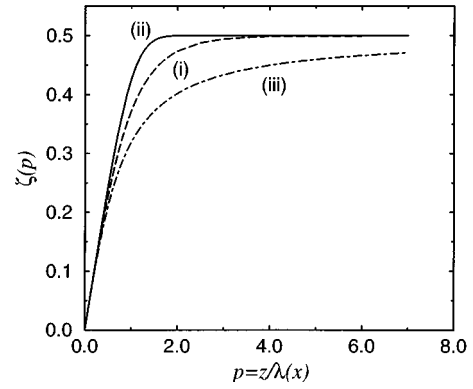


FIG. 1. Normalized temperature profile $\zeta(p)$ for the three different cases: (i) $K=1.00587$ and $A=1.01771$, (ii) $K=0$ and $A=2.13622$, and (iii) $A=0$ $K=\pi/2$.

$\text{Ra} > 10^8$ that coincide with each other. A comparison of this common profile with Fig. 1 suggests that it corresponds to $K \neq 0$ and $A \neq 0$. If the normalized temperature profile does remain the same over a substantial range of Ra , we have Eq. (13) with $A(K)/K$ being constant over the same range. Since $\text{Nu} \sim \text{Ra}^{2/7}$, this implies $\gamma_0 L^2/\kappa \sim \text{Ra}^{4/7} \ln \text{Ra}$. If a straight line is fitted to a log-log plot of $\gamma_0 L^2/\kappa$ versus Ra , the slope obtained will depend on the range of Ra . An example of such a plot for $10^8 < \text{Ra} < 10^{10}$ (the range of Ra covered in the experiment in Ref. [13]) is shown in Fig. 2. The exponent so obtained is 0.62, which is in better agreement with the experimental result of 0.66 ± 0.01 [13]. It is thus interesting to check whether the normalized temperature profile remains the same over the range of Ra covered and whether the profile corresponds to $K \neq 0$ and $A \neq 0$.

I have presented an analysis of the interaction of the thermal and velocity boundary layers for the general case of nonuniform shear. The relation between the heat flux and shear rate depends on the shape of the temperature profile. However, the same $2/7$ Nu scaling has been observed irrespective of whether the shear rate scales like Nu^3 [15] or not [13]. This implies that the cause of the nonclassical scaling

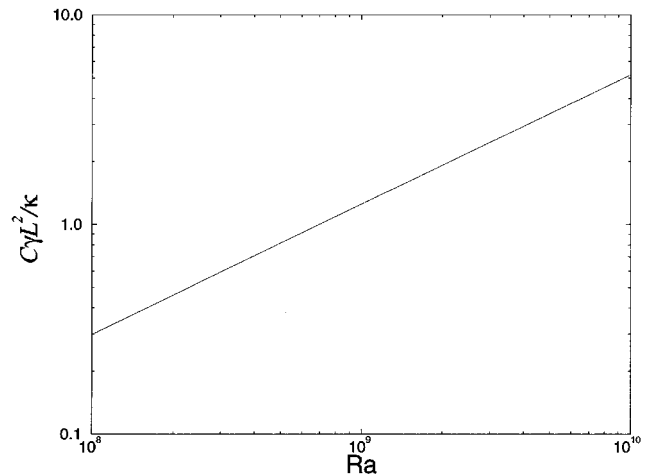


FIG. 2. Plot of $\gamma_0 L^2/\kappa$ versus Ra using Eq. (13) with $\text{Nu} \sim \text{Ra}^{2/7}$ and $A(K)/K$ taken to be constant. A good straight line can be fitted in the log-log plot and the slope obtained is 0.62, which agrees better with Eq. (5). C is an arbitrary constant.

of Nu is more general than that given in Ref. [8] and a full understanding remains to be obtained.

I thank L.P. Kadanoff for his helpful comments and K.-Q. Xia for discussing experimental results with me prior to publication. I would also like to acknowledge discussions

with B.I. Shraiman while we were at the Aspen Center for Physics. This work was partially supported by the Institute of Mathematical Sciences at the Chinese University of Hong Kong and by the Hong Kong Research Grants Council (Grant No. 458/95P).

-
- [1] F. Heslot, B. Castaing, and A. Libchaber, *Phys. Rev. A* **36**, 5870 (1987); X.Z. Wu, Ph.D. thesis, University of Chicago, 1991 (unpublished).
- [2] W. V. R. Malkus, *Proc. R. Soc. London, Ser. A* **225**, 185 (1954); L. N. Howard, *J. Fluid Mech.* **17**, 405 (1963).
- [3] M. Sano, X.Z. Wu, and A. Libchaber, *Phys. Rev. A* **40**, 6421 (1989).
- [4] S. Chandrasekhar, *Hydrodynamic and Hydromagnetic Stability* (Dover, New York, 1981).
- [5] A. Belmonte, A. Tilgner, and A. Libchaber, *Phys. Rev. E* **50**, 269 (1994); see also A. Belmonte, Ph.D. thesis, Princeton University, 1994 (unpublished).
- [6] B. Castaing *et al.* *J. Fluid Mech.* **204**, 1 (1989).
- [7] Z.-S. She, *Phys. Fluids A* **1**, 911 (1989).
- [8] B. I. Shraiman and E. D. Siggia, *Phys. Rev. A* **42**, 3650 (1990).
- [9] Hot and cold jets carrying a substantial amount of heat are observed near the sidewalls in the two-dimensional numerical simulations by E. E. DeLuca, J. Werne, R. Rosner, and F. Cattaneo, *Phys. Rev. Lett.* **64**, 2370 (1990); **67**, 3519 (1991).
- [10] T. H. Solomon and J. P. Gollub, *Phys. Rev. Lett.* **64**, 2382 (1990); *Phys. Rev. A* **43**, 6683 (1991).
- [11] A. Tilgner, A. Belmonte, and A. Libchaber, *Phys. Rev. E* **47**, R2253 (1993).
- [12] A. Belmonte, A. Tilgner, and A. Libchaber, *Phys. Rev. Lett.* **70**, 4067 (1993).
- [13] Y.-B. Xin, K.-Q. Xia, and P. Tong, *Phys. Rev. Lett.* **77**, 1266 (1996).
- [14] F. Chilla, S. Ciliberto, and C. Innocenti, *Europhys. Lett.* **22**, 681 (1993).
- [15] J. Werne, *Phys. Rev. E* **48**, 1020 (1993).
- [16] The fact that the heat transport carried by the thermal plumes can only be included if γ is position dependent has also been noted in Appendix D of Ref. [5].
- [17] This well-known result from classical boundary layer theory [see for example, H. Schlichting, *Boundary-Layer Theory* (McGraw-Hill, New York, 1968), Chap. VIII(b)] was pointed out to me by B. Castaing. He also pointed out the derivation of Eq. (12).